Int J Clin Exp Pathol 2020;13(8):2041-2049
www.ijcep.com /ISSN:1936-2625/IJCEP0110924

Original Article

Protective effects of ferroptosis inhibition on high fat diet-induced liver and renal injury in mice

Yinli Luo[1*], Hongjin Chen[2*], Hui Liu[2], Wenjing Jia[2], Jueqian Yan[2], Wenting Ding[2], Yali Zhang[2], Zhongxiang Xiao[3], Zaisheng Zhu[1]

[1]Department of Geriatric Medicine, First Affiliated Hospital of Wenzhou Medical University, Wenzhou 325035, Zhejiang, China; [2]Chemical Biology Research Center, School of Pharmaceutical Sciences, Wenzhou Medical University, Wenzhou 325035, Zhejiang, China; [3]Affiliated Yueqing Hospital, Wenzhou Medical University, Wenzhou 325600, Zhejiang, China. [*]Equal contributors.

Received March 15, 2020; Accepted April 16, 2020; Epub August 1, 2020; Published August 15, 2020

Abstract: As a complex and highly prevalent global public health problem, obesity is associated with multiple diseases, including liver and renal injury. As an iron-dependent form of cell death, ferroptosis is different from apoptosis and necrosis, which has been reported to participate in pathologic processes of many diseases. However, whether ferroptosis is involved in obesity-induced liver and renal injury remains unclear. Male C57BL/6 mice were fed with high-fat diet (HFD) or control diet for 16 weeks and treated with 5 mg/kg or 10 mg/kg ferroptosis inhibitor, ferrostatin-1 (Fer-1), for the last 8 weeks with results indicating that glutathione peroxidase 4 (GPX4) gene expression decreased in the liver and renal tissue of obese mice. Additionally, Fer-1 pretreatment prevented the obesity-induced decline of GPX4. More importantly, Fer-1 treatment attenuated HFD-induced pathological and functional impairment, fibrosis, inflammatory cell infiltration, and inflammatory cytokine expression in liver and renal tissues. In short, our results indicate that obesity can induce ferroptosis and ferroptosis inhibitor, Fer-1, thereby inhibiting obesity-induced liver and renal injury in mice. The study provides a new therapeutic direction for the complications of obesity.

Keywords: Ferroptosis, obesity, liver, renal, fibrosis

Introduction

Obesity is a serious public health problem to not only in Western countries but also in China. Epidemiologists predicted that the global obesity prevalence will reach 18% in men and 21% in women by 2025 [1]. Although intense efforts have been conducted to control obesity, no improvement was obtained in terms of the high prevalence of obesity [2, 3]. Excess fat deposition is often responsible for type-2 diabetes mellitus, hypertension, cancer, cardiovascular diseases, chronic kidney disease, and fatty liver disease, helping explain evidence showing an association between obesity and structural as well as functional changes in the liver and kidney in both humans and animal models [4-7] [5, 8-10]. Additionally, the fundamental mechanisms of obesity-induced liver and renal injury are involved in lipotoxicity, inflammation, and increased oxidative stress [11, 12]. Apart from these mechanisms, whether other mechanisms are involved, should be explored.

Ferroptosis is an iron-dependent form of oxidative programmed cell death characterized by glutathione peroxidase 4 (GPX4) inactivation, glutathione depletion, and increased lipid hydroperoxide levels [13, 14]. Although most previous studies focused more on ferroptosis in cancer, more recent publications indicated that ferroptosis is involved in abundant pathologic processes such as acute kidney injury, liver fibrosis, APAP-induced liver injury, neurotoxicity, and neurodegenerative diseases [15-20]. However, whether the effects of ferroptosis are involved in the development of obesity complications remains unclear. In our current study, ferrostatin-1 (Fer-1), a ferroptosis inhibitor, was employed as a probe to study the role of ferroptosis in obesity-induced liver and renal injury in mice.

Materials and methods

Reagents

Fer-1 (#S7243) was purchased from Selleck Chemicals (Houston, TX, USA).

Animals

Twenty-eight male C57BL/6 mice weighing 18-22 g were obtained from the Animal Center of Wenzhou Medical University. The mice were housed with *ad libitum* access to food and water at 22 ± 2.0°C and 50 ± 5% humidity with a 12-h: 12-h light/dark cycle in an environmentally controlled room. The animal care and experimental procedures complied with the 'The Detailed Rules and Regulations of Medical Animal Experiments Administration and Implementation' (Order No. 1998-55, Ministry of Public Health, China) and 'Ordinance in Experimental Animal Management' (Order No. 1998-02, Ministry of Science and Technology, China) and were approved by the Wenzhou Medical University Animal Policy and Welfare Committee (Approval Document No. wydw-2017-0140).

Mice were randomly divided into four groups: 1) control (CON) group: mice in this group were fed with standard animal chow (10 kcal.% fat, 20 kcal.% protein and 70 kcal.% carbohydrate; Cat. #MD12031; MediScience Diets Co. LTD, Yangzhou, China) for 16 weeks; 2) high fat diet (HFD) group: mice in this group were fed with HFD (60 kcal.% fat, 20 kcal.% protein and 20 kcal.% carbohydrate; Cat. #MD12033; MediScience Diets Co. LTD, Yangzhou, China) for 16 weeks; 3) HFD+Fer-1 5 group: mice in this group were fed with HFD for 16 weeks and intraperitoneally injected with 5 mg/kg Fer-1 every two days for the last 8 weeks; 4) HFD+Fer-1 10 group: mice in this group were fed with HFD for 16 weeks and intraperitoneally injected with 10 mg/kg Fer-1 every two days for the last 8 weeks. Specifically, the control group and HFD group mice were intraperitoneally injected with vehicle (CMC-Na) every two days for the last 8 weeks. Body weight was recorded weekly. Additionally, mice were anaesthetized with chloral hydrate after being fasted for 6 h. Blood was sampled by the cardiac puncture method. Renal and liver tissues were dissected and snap-frozen in liquid nitrogen for RNA extraction or prepared for histology.

Oral glucose tolerance test

Mice were fasted for 12 h, followed by the delivery of glucose (2 g/kg body weight) by oral gavage. Following that, tail vein blood glucose was detected at indicated time points (0, 15, 30, 60, 90 and 120 min) using a glucometer (Onetouch Ultravue, Shanghai, China).

Biochemical analysis of serum samples

Collected blood samples were centrifuged at 3000 rpm for 15 min to obtain serum, with the serum levels of TG, TCH, ALT, AST, BUN, ALB and hydroxyproline being determined according to the instructions (Nanjing Jiancheng Bioengineering Institute, Nanjing, China).

RT-qPCR

After being extracted from renal and liver tissues (15-20 mg) using TRIzol (Life Technologies, Carlsbad, CA, USA), total RNA concentration was measured in duplicate applying SpectraMaxM5 Microplate Reader (Molecular Devices, Sunnyvale, CA, USA), with the purity of the samples being estimated by the OD ratio (A260/A280, ranging within 1.8-2.2). Reverse transcription PCR was performed applying M-MLV Platinum RT-qPCR kit (Invitrogen, Shanghai, China), and real-time qPCR was carried out using the Eppendorf Real plex 4 instrument (Eppendorf, Hamburg, Germany). Primers for genes applied in this study were obtained from Life Technologies (Carlsbad, CA, USA). The relative amount of each gene was normalized to the amount of β-actin. The primer sequences used are shown as follows: mouse TNF-α forward primer, 5'-TGATCCGCGACGTGGAA-3'; mouse TNF-α reverse primer, 3'-ACCGCCTGGAGTTCTGGAA-5'; mouse IL-6 forward primer, 5'-GAGGATACCACTCCCAACAGACC-3'; mouse IL-6 reverse primer, 3'-AAGTGCATCATCGTTGTTCATACA-5'; mouse TGF-β forward primer, 5'-TGACGTCACTGGAGTTGTACGG-3'; mouse TGF-β reverse primer, 3'-GGTTCATGTCATGGATGGTGC-5'; mouse Col-IV forward primer, 5'-CGTACCTGCTGACTATCTTCA-3'; mouse Col-IV reverse primer, 3'-GTTGGACACTGGACGCTA-5'; mouse β-actin forward primer, CCGTGAAAAGATGACCCAGA; mouse β-actin reverse primer, TACGACCAGAGGCATACAG.

Histologic and Immunohistochemical (IHC) analysis

Renal and liver tissues were fixed in 4% paraformaldehyde solution, with tissues being then embedded in paraffin and cut into 5 μm sections which were stained with H&E or Masson's trichrome staining using standard protocol and viewed under a light microscope (200× amplification). The ratio of fibrosis was qualified by an image analysis on Masson's trichrome staining of the liver and kidney sections of the seven mice in each group. At 200× magnification, the Image-pro Plus (Media Cybernetics Inc., Silver Spring, MD, USA) software was applied to quantify the amount of tissue (red signal) and collagen (blue signal) inside the liver and kidney tissues of 10 randomly chosen frames, with the ratio of collagen to liver or kidney tissue being recorded for each specimen.

For tissue immunostaining, sections were deparaffinized, rehydrated, and incubated with primary F4/80 antibody, followed by application of HRP-conjugated secondary antibody and diaminobenzidine for detection. The sections were viewed by a light microscope (200× amplification). At 200× magnification, the area of the staining signal (F4/80, anti-F4/80 antibody, Santa Cruz Biotechnology, U.S.A) of ten random fields was measured using the Image-pro Plus software (Media Cybernetics Inc., Silver Spring, MD, USA), with the percentage expression of F4/80 was recorded for each specimen.

Statistical analysis

The statistical significance of differences between groups was obtained by the Student's t-test in GraphPad Pro 5.0 (GraphPad, San Diego, CA, USA). Results are expressed as mean ± SEM. Differences were considered to be significant at $^{\#}P<0.05$, $^{\#\#}P<0.01$, $^{\#\#\#}P<0.001$ *v.s.* CON group; $^{*}P<0.05$; $^{**}P<0.01$, $^{***}P<0.001$ *v.s.* HFD group.

Results

Without effect on HFD-induced obesity, Fer-1 improves the GPX4 mRNA level in renal and liver tissue in obese mice

Figure 1A shows the chemical structure of Fer-1. HFD-fed mice became markedly obese with a body weight over 47 g on average at the end of the animal experiment. However, either 5 mg/kg or 10 mg/kg Fer-1 treatment for 8 weeks, compared with HFD group, resulted in no significant differences in mice body weight (**Figure 1B**). Meanwhile, Fer-1 treatment also showed no improvement in terms of obesity-induced glucose tolerance (**Figure 1C**, **1D**). In short, these results indicate that Fer-1 does not play a role in the development of obese mice.

The mRNA level of GPX4, a marker of ferroptosis [13], was studied to determine the effect of Fer-1 on ferroptosis in obese mice. As shown in **Figure 1E** and **1F**, GPX4 gene level was decreased obviously in obese liver (**Figure 1E**) and kidney (**Figure 1F**) tissues. Mice treated with Fer-1 increased the GPX4 mRNA level both in liver (**Figure 1E**) and kidney (**Figure 1F**) tissues. Thus, these results indicate that Fer-1 can contribute to attenuating HFD-induced ferroptosis both in liver and renal tissues.

Fer-1 protects against HFD-induced liver and renal injury

Next, the protective effect of Fer-1 on obesity-induced liver and renal injury is examined. HFD mice, compared with con mice, showed increased serum levels of hallmarks of liver function injury (ALT, AST, Hydroxyproline) and renal function injury (CK, BUN and ALB) (**Figure 2A-C**, **2E-G**). However, these markers were reduced in HFD mice treated with Fer-1 at 5 or 10 mg/kg effectively. Additionally, the histopathology of the liver and kidney was examined to determine Fer-1's effect on HFD-induced pathologic damage. Staining with H&E demonstrated that the liver sections from the HFD group, when compared with the con group, showed significant structural abnormalities and lipid accumulation, whereas those in the Fer-1 treated groups did not (**Figure 2D**). Kidney shows similar improvements of histological abnormalities as well. Staining with H&E showed the kidney sections from the HFD group exhibited glomerular shrinkage and mesangial matrix expansion, whereas these changes were not as evident in the con and Fer-1 treated groups (**Figure 2H**). In short, these data show that HFD is responsible for liver and renal tissue damage, but Fer-1 can attenuate HFD-induced tissue injury.

Fer-1 protects against HFD-induced liver and renal fibrosis

Masson trichrome staining was conducted to explore the role of Fer-1 in liver and renal fibro-

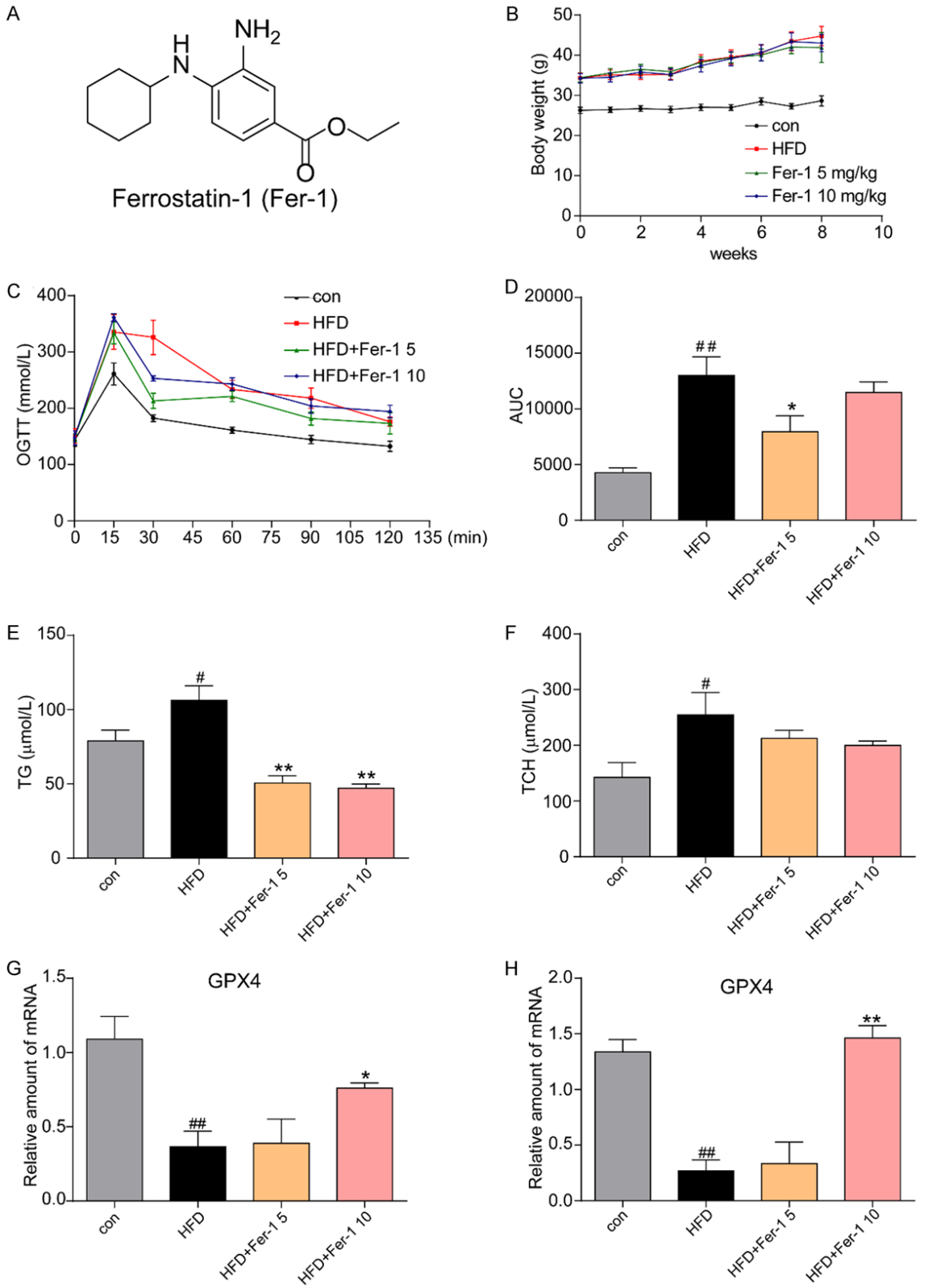

Figure 1. Fer-1 does not attenuate obesity but improves the GPX4 mRNA level in liver and kidney. (A) The chemical structure of Fer-1. (B) Weekly body weight of mice after HFD over 8 weeks. (C, D) The blood glucose level of OGTT. (E) Serum levels of TG presented in μM. (F) Serum levels of TCH presented in μmol/L. (G, H) RT-qPCR assay showed the mRNA levels of GPX4 in liver (G) and renal (H) tissue. mRNA values were normalized to housekeeping gene β-actin. Data are presented as mean ± SEM, n=7 in each group. $^{\#}P<0.05$, $^{\#\#}P<0.01$, *vs* con group; $*P<0.05$, $**P<0.01$, *vs* HFD group.

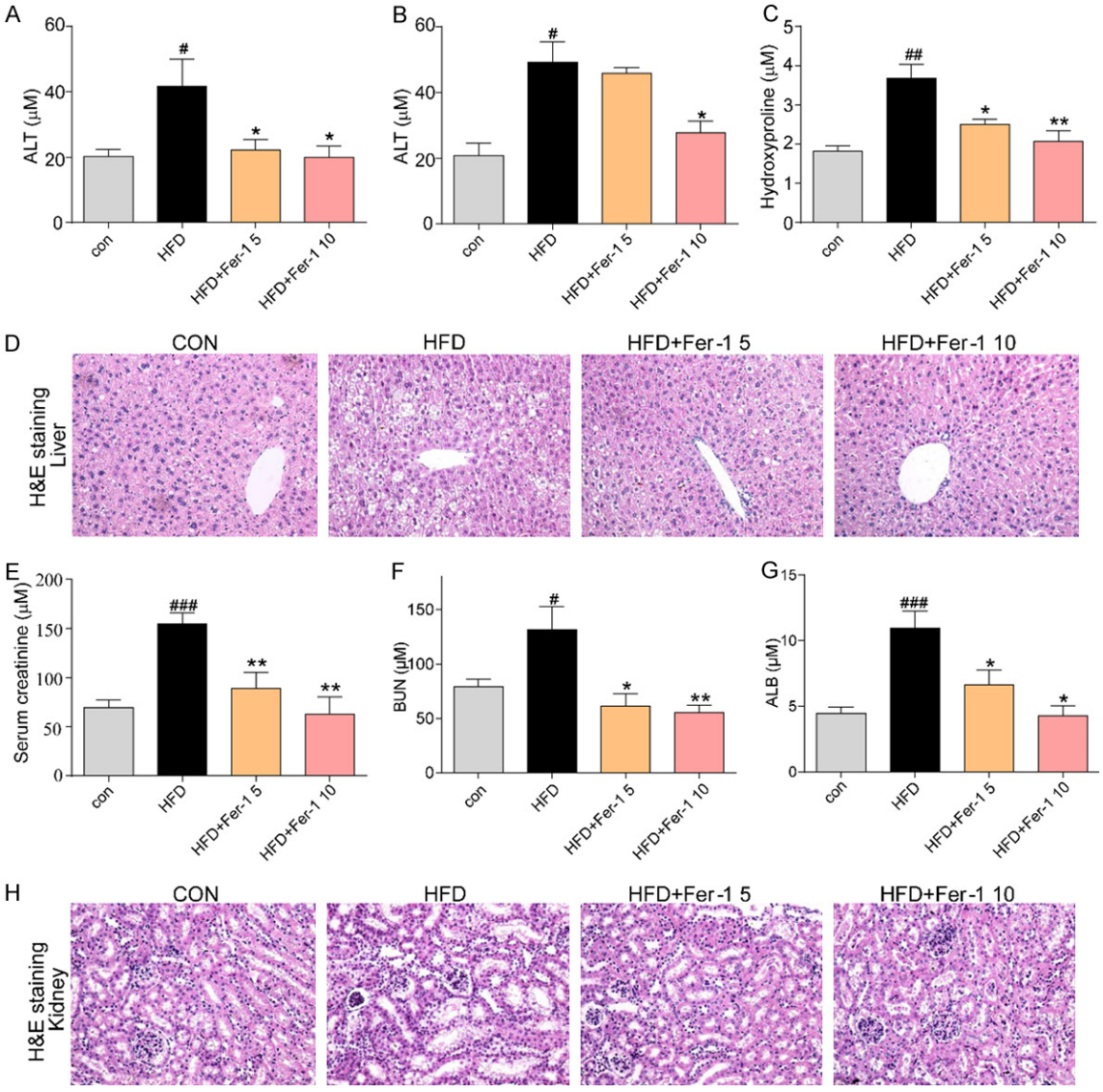

Figure 2. Fer-1 protects against HFD-induced renal and liver injury. (A-C) Serum levels of ALT (A), AST (B), and hydroxyproline (C) presented in μM. (D) Representative histopathologic changes in liver tissue detected with H&E stain (×200). (E-G) Serum levels of creatinine (E), BUN (F) and ALB (G) presented in μM. (H) Representative histopathologic changes in renal tissue detected with H&E stain (×200). Data are presented as mean ± SEM, n=7 in each group. $^{\#}P<0.05$, $^{\#\#}P<0.01$, *vs* con group; $^{*}P<0.05$, $^{**}P<0.01$, *vs* HFD group.

sis. As shown in **Figure 3A** and **3D**, Masson staining for collagen suggested that HFD, compared with mice on a normal diet, obviously induced liver and renal fibrosis. However, HFD mice that were administered Fer-1 showed a reduced fibrosis both in the liver and the kidney. Additionally, the quantitative result of Masson staining, shown in **Figure 3B** and **3E**, further indicated that Fer-1 reduced HFD-induced collagen deposition in liver and renal tissue. Furthermore, the gene expression of fibrosis markers, TGF-β and Col-IV, was elevated in liver (**Figure 3C**) and renal (**Figure 3F**) tissue in HFD mice. Fer-1 dose-dependently reduced the TGF-β and Col-IV mRNA level. In short, these results indicate that Fer-1 can contribute to attenuating HFD-induced fibrosis in liver and renal tissue.

Fer-1 protects against HFD-induced liver and renal inflammation

Inflammation plays an important role in the development of HFD-induced tissue injury [11].

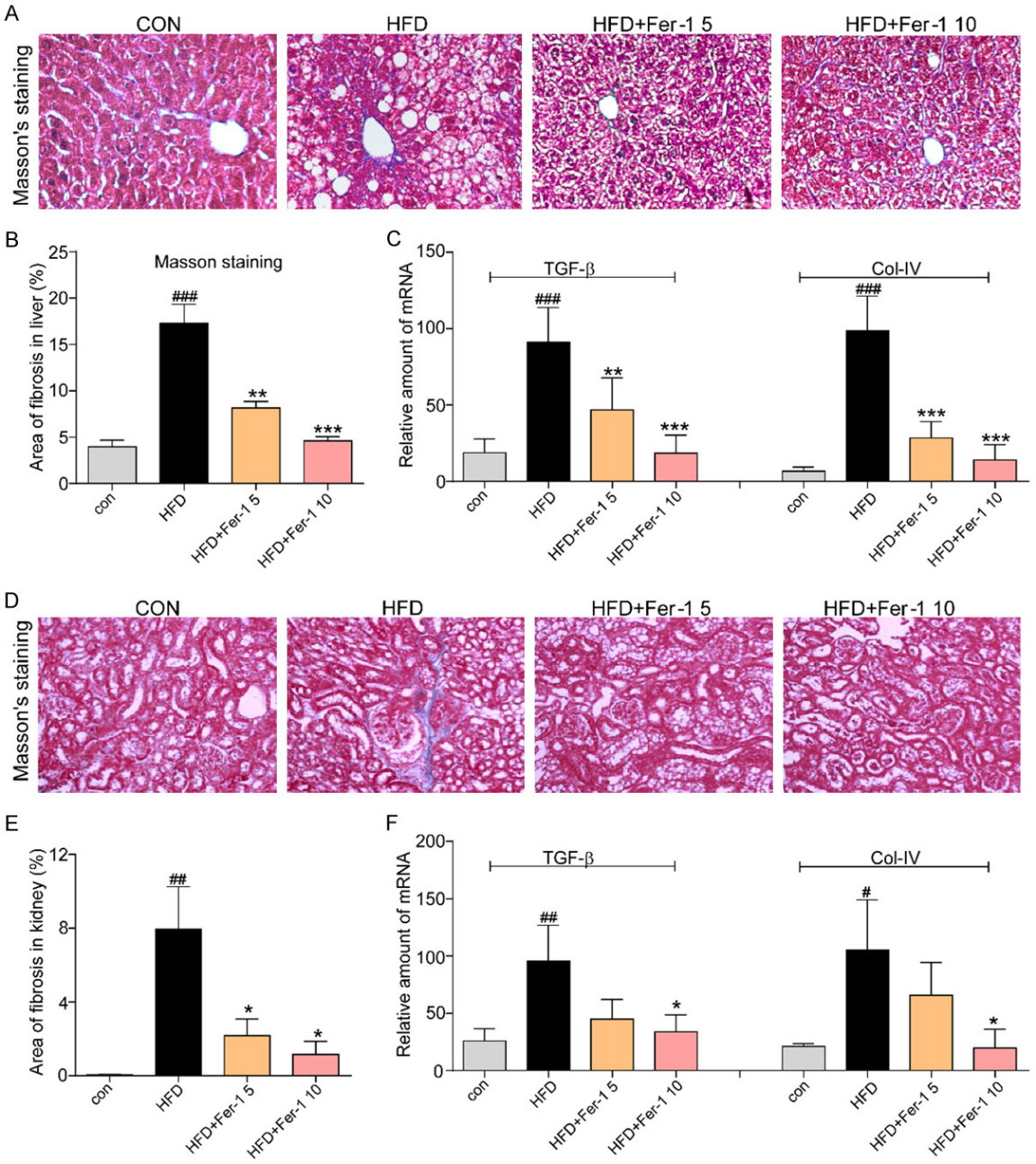

Figure 3. Fer-1 protects against HFD-induced liver and renal tissue fibrosis. A. Masson's Trichrome staining was used as index of liver fibrosis. B. Quantification for the area of fibrosis in liver tissues detected by Masson's Trichirome stain. C. RT-qPCR assay showed the mRNA levels of markers (TGF-β and Col-IV) of fibrosis in liver. mRNA values were normalized to housekeeping gene β-actin. D. Masson's Trichrome staining was used as index of liver fibrosis. E. Quantification for the area of fibrosis in liver tissues detected by Masson's trichrome staining. F. RT-qPCR assay showed the mRNA levels of markers (TGF-β and Col-IV) of fibrosis in kidney. mRNA values were normalized to housekeeping gene β-actin. Data are presented as mean ± SEM, n=7 in each group. $^{\#}P<0.05$, $^{\#\#}P<0.01$, *vs* con group; $^{*}P<0.05$, $^{**}P<0.01$, *vs* HFD group.

IHC staining showed that pretreatment with Fer-1 at 5 or 10 mg/kg decreased significantly HFD-induced F4/80 positive cell infiltration in liver and kidney tissues (**Figure 4A** and **4D**). The quantitative result of IHC staining, as shown in **Figure 4B** and **4E**, further indicated that the increased percentage of F4/80 positive cells induced by HFD was inhibited by Fer-1 in liver and renal tissues. Real-time PCR analysis demonstrated that the amounts of two inflammato-

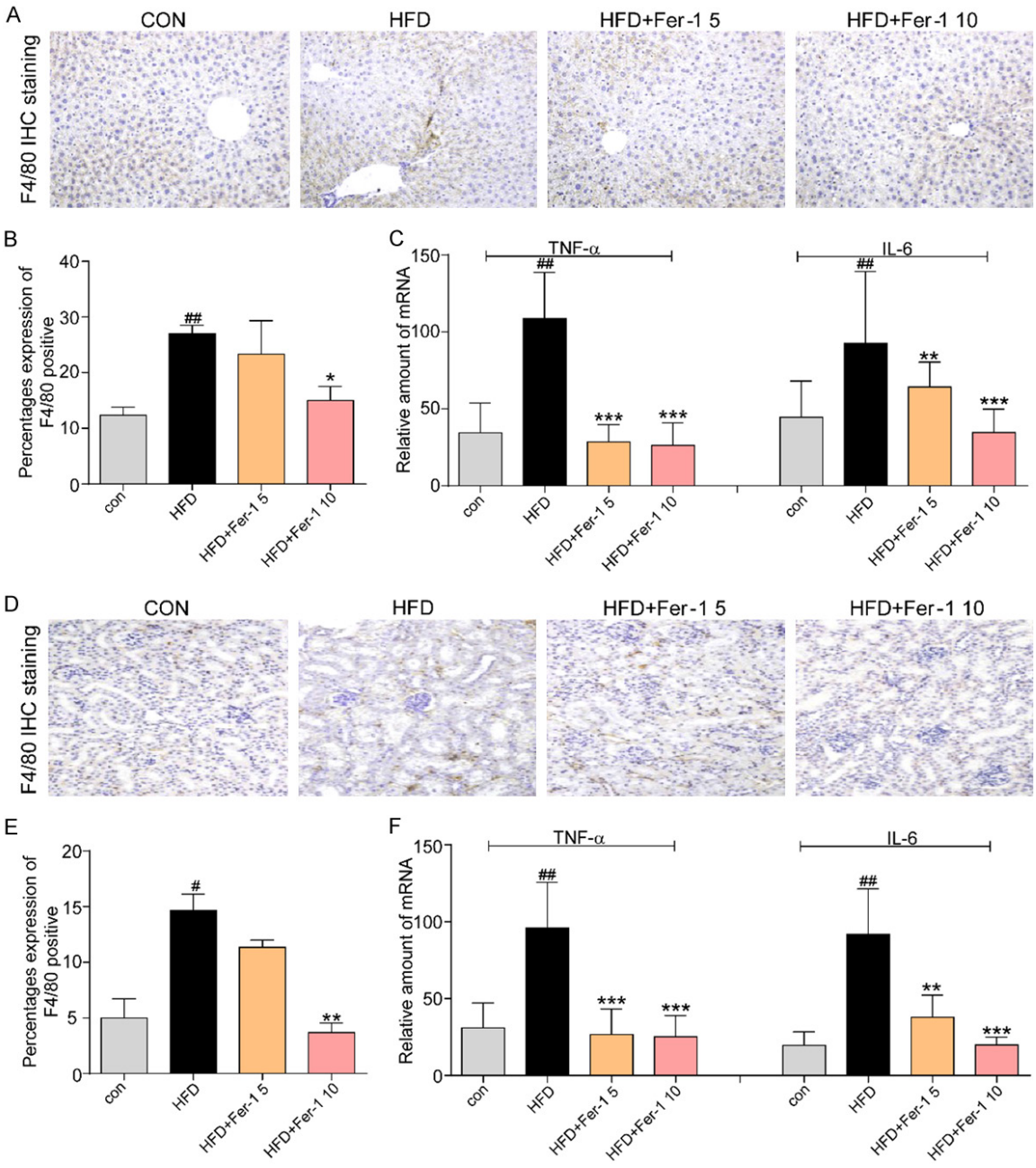

Figure 4. Fer-1 protects against HFD-induced liver and renal tissue inflammation. A. Representative image of immunohistochemical staining of F4/80 in liver tissue sections. B. Quantification for the percentages expression of F4/80 positive cells in liver. C. RT-qPCR assay shows the mRNA levels of markers (TNF-α and IL-6) involved in the inflammatory response in liver, with mRNA values being normalized to housekeeping gene β-actin. D. Representative image of immunohistochemistry staining of F4/80 in renal tissue sections. E. Quantification for the percentages expression of F4/80 positive cells in kidney. F. RT-qPCR assay shows the mRNA levels of markers (TNF-α and IL-6) of inflammatory response in kidney, with mRNA values being normalized to housekeeping gene β-actin. Data are presented as mean ± SEM, n=7 in each group. $^{\#}P<0.05$, $^{\#\#}P<0.01$, *vs* con group; $^{*}P<0.05$, $^{**}P<0.01$, *vs* HFD group.

ry factors, TNF-α and IL-6, were increased markedly in HFD group mice but this situation was reversed by Fer-1 both in liver (**Figure 4C**) and renal (**Figure 4F**) tissues.

Discussion

Obesity is considered as an increasingly major public health concern worldwide. Researches

on ways of slowing the development of obesity have traditionally focused on dietary as well as lifestyle modifications, such as restricting caloric intake and increasing physical activity [21]. However, many patients, due to difficulty with adherence and physiologic adaptation of the body in response to weight loss, haven't achieved long-lasting benefits. Chronic obesity can cause various complications and tissue injury, accompanied by low-grade chronic inflammation, fibrosis, and oxidative stress [12]. Our study shows that HFD-induced liver and renal tissue pathology and functional impairment, decline of GPX4, inflammatory cell infiltration, expression of inflammatory cytokines, fibrosis, and oxidative stress.

Dependent upon intracellular iron, ferroptosis is morphologically, biochemically, and genetically distinct from apoptosis and necrosis [13], which is triggered by disturbed redox homeostasis, iron overload, and increased lipid peroxidation [14]. Many publications have revealed that ferroptosis was involved in various pathologic processes. For example, in cancer, ferroptosis may act as a tumor suppressor regulated by P53 [16]. In the mouse model of acute kidney injury induced by lipid-oxidation/ischemic/nephrotoxic folic acid/rhabdomyolysis/cisplatin, ferroptosis is involved in the progression and aggravation of disease [19, 20, 22-24]. Additionally, ferroptosis was also reported to participate in several liver diseases, such as liver fibrosis, acetaminophen-induced cell death, alcoholic-induced steatohepatitis, and LPS/galactosamine-induced liver injury [17, 25-27]. In our current study, we found that Fer-1, a ferroptosis inhibitor, attenuates obesity-induced liver and renal injury, including tissue inflammation and fibrosis. Thus, our results indicate that ferroptosis participates in obesity-induced liver and renal injury.

Conclusions

Our current research shows that the GPX4 level was decreased in obesity-induced damaged liver and renal tissues in mice, indicative of obesity-induced ferroptosis in liver and renal tissue. However, pretreatment with Fer-1 reversed the effects induced by obesity. Further, Fer-1 treatment inhibited HFD-induced tissue injury, inflammation, and fibrosis in liver and renal tissues. Although the underlying mechanism of ferroptosis induces inflammation and fibrosis, and how hyperlipemia activates ferroptosis, are not clear in this article, our study provides a new therapy target for obesity complications.

Acknowledgements

This study was supported by Zhejiang Provincial Natural Science Funding (LY15H250002 to Z.Z.), and Public Welfare Science and Technology Project of Wenzhou (Y20150176 to Z.Z. and Y20180594 to Z.X.).

Disclosure of conflict of interest

None.

Abbreviations

ALB, albumin; ALT, alanine aminotransferase; AST, aspartate aminotransferase; CON, control; Fer-1, ferrostatin-1; H&E, hematoxylin and eosin; HFD, high fat diet; IHC, immunohistochemical; RT-qPCR, real-time quantitative PCR; TCH, total cholesterol; TG, total triglyceride.

Address correspondence to: Zaisheng Zhu, Department of Geriatric Medicine, The First Affiliated Hospital of Wenzhou Medical University, Wenzhou 325035, Zhejiang, China. Tel: +86-13857734265; E-mail: zhuzaisheng@wmu.edu.cn; Zhongxiang Xiao, Affiliated Yueqing Hospital, Wenzhou Medical University, Wenzhou 325600, Zhejiang, China. Tel: +86-13736316636; E-mail: xiangzi198155@163.com

References

[1] NCD Risk Factor Collaboration (NCD-RisC). Trends in adult body-mass index in 200 countries from 1975 to 2014: a pooled analysis of 1698 population-based measurement studies with 19.2 million participants. Lancet 2016; 387: 1377-1396.

[2] Obesity: preventing and managing the global epidemic. Report of A WHO consultation. World Health Organ Tech Rep Ser 2000; 894: i-xii, 1-253.

[3] Heymsfield SB and Wadden TA. Mechanisms, pathophysiology, and management of obesity. N Engl J Med 2017; 376: 1492.

[4] Kamal R, Correia ML, Haynes WG and Mark AL. Obesity-associated hypertension: new insights into mechanisms. Hypertension 2005; 45: 9-14.

[5] Eknoyan G. Obesity, diabetes, and chronic kidney disease. Curr Diab Rep 2007; 7: 449-453.

[6] Bianchini F, Kaaks R and Vainio H. Overweight, obesity, and cancer risk. Lancet Oncol 2002; 3: 565-574.
[7] Marchesini G, Moscatiello S, Di DS and Forlani G. Obesity-associated liver disease. J Clin Endocrinol Metab 2008; 93: s74-s80.
[8] Silverman JF, O'Brien KF, Long S, Leggett N, Khazanie PG, Pories WJ, Norris HT and Caro JF. Liver pathology in morbidly obese patients with and without diabetes. Am J Gastroenterol 1990; 85: 1349-55.
[9] Wu B, Xiao Z, Zhang W, Chen H, Liu H, Pan J, Cai X, Liang G, Zhou B, Shan X and Zhang Y. A novel resveratrol-curcumin hybrid, a19, attenuates high fat diet-induced nonalcoholic fatty liver disease. Biomed Pharmacother 2019; 110: 951-960.
[10] Ditonno P and Lucarelli G. Obesity in kidney transplantation affects renal function but not graft and patient survival. Transplant Proc 2011; 43: 367-372.
[11] Esser N, Legrand-Poels S, Piette J, Scheen AJ and Paquot N. Inflammation as a link between obesity, metabolic syndrome and type 2 diabetes. Diabetes Res Clin Pract 2014; 105: 141-150.
[12] Fernándezsánchez A, Madrigalsantillán E, Bautista M, Esquivelsoto J, Moralesgonzález A, Esquivelchirino C, Durantemontiel I, Sánchezrivera G, Valadezvega C and Moralesgonzález JA. Inflammation, oxidative stress, and obesity. Int J Mol Sci 2011; 12: 3117-32.
[13] Dixon S, Lemberg K, Lamprecht M, Skouta R, Zaitsev E, Gleason C, Patel D, Bauer A, Cantley A and Yang WS. Ferroptosis: an iron-dependent form of nonapoptotic cell death. Cell 2012; 149: 1060-1072.
[14] Cao JY and Dixon SJ. Mechanisms of ferroptosis. Cell Mol Life Sci 2016; 73: 2195-2209.
[15] Wenzel SE, Tyurina YY, Zhao J, St Croix CM, Dar HH, Mao G, Tyurin VA, Anthonymuthu TS, Kapralov AA, Amoscato AA, Mikulska-Ruminska K, Shrivastava IH, Kenny EM, Yang Q, Rosenbaum JC, Sparvero LJ, Emlet DR, Wen X, Minami Y, Qu F, Watkins SC, Holman TR, VanDemark AP, Kellum JA, Bahar I, Bayır H and Kagan VE. PEBP1 Wardens ferroptosis by enabling lipoxygenase generation of lipid death signals. Cell 2017; 171: 628-641, e26.
[16] Perlman AS, Chevalier JM, Wilkinson P, Liu H, Parker T, Levine DM, Sloan BJ, Gong A, Sherman R and Farrell FX. Serum inflammatory and immune mediators are elevated in early stage diabetic nephropathy. Ann Clin Lab Sci 2015; 45: 256-63.
[17] Sui M, Jiang X, Chen J, Yang H and Zhu Y. Magnesium isoglycyrrhizinate ameliorates liver fibrosis and hepatic stellate cell activation by regulating ferroptosis signaling pathway. Biomed Pharmacother 2018; 106: 125-133.
[18] Tuo QZ, Lei P, Jackman KA, Li XL, Xiong H, Li XL, Liuyang ZY, Roisman L, Zhang ST and Ayton S. Tau-mediated iron export prevents ferroptotic damage after ischemic stroke. Mol Psychiatry 2017; 22: 1520-1530.
[19] Mishima E, Sato E, Ito J, Yamada KI, Suzuki C, Oikawa Y, Matsuhashi T, Kikuchi K, Toyohara T, Suzuki T, Ito S, Nakagawa K and Abe T. Drugs repurposed as antiferroptosis agents suppress organ damage, including AKI, by functioning as lipid peroxyl radical scavengers. J Am Soc Nephrol 2020; 31: 280-296.
[20] Guerrero-Hue M, Garcia-Caballero C, Palomino-Antolin A, Rubio-Navarro A, Vazquez-Carballo C, Herencia C, Martin-Sanchez D, Farre-Alins V, Egea J, Cannata P, Praga M, Ortiz A, Egido J, Sanz AB and Moreno JA. Curcumin reduces renal damage associated with rhabdomyolysis by decreasing ferroptosis-mediated cell death. FASEB J 2019; 33: 8961-8975.
[21] Gadde KM, Martin CK, Berthoud HR and Heymsfield SB. Obesity: pathophysiology and management. J Am Coll Cardiol 2018; 71: 69-84.
[22] Friedmann Angeli JP, Schneider M, Proneth B, Tyurina YY, Tyurin VA, Hammond VJ, Herbach N, Aichler M, Walch A, Eggenhofer E, Basavarajappa D, Radmark O, Kobayashi S, Seibt T, Beck H, Neff F, Esposito I, Wanke R, Forster H, Yefremova O, Heinrichmeyer M, Bornkamm GW, Geissler EK, Thomas SB, Stockwell BR, O'Donnell VB, Kagan VE, Schick JA and Conrad M. Inactivation of the ferroptosis regulator Gpx4 triggers acute renal failure in mice. Nat Cell Biol 2014; 16: 1180-1191.
[23] Muller T, Dewitz C, Schmitz J, Schroder AS, Brasen JH, Stockwell BR, Murphy JM, Kunzendorf U and Krautwald S. Necroptosis and ferroptosis are alternative cell death pathways that operate in acute kidney failure. Cell Mol Life Sci 2017; 74: 3631-3645.
[24] Martin-Sanchez D, Ruiz-Andres O, Poveda J, Carrasco S, Cannata-Ortiz P, Sanchez-Nino MD, Ruiz Ortega M, Egido J, Linkermann A, Ortiz A and Sanz AB. Ferroptosis, but not necroptosis, is important in nephrotoxic folic acid-induced AKI. J Am Soc Nephrol 2017; 28: 218-229.
[25] Lorincz T, Jemnitz K, Kardon T, Mandl J and Szarka A. Ferroptosis is involved in acetaminophen induced cell death. Pathol Oncol Res 2015; 21: 1115-1121.
[26] Zhou Z, Ye TJ, Bonavita G, Daniels M, Kainrad N, Jogasuria A and You M. Adipose-specific lipin-1 overexpression renders hepatic ferroptosis and exacerbates alcoholic steatohepatitis in mice. Hepatol Commun 2019; 3: 656-669.
[27] Kong Z, Liu R and Cheng Y. Artesunate alleviates liver fibrosis by regulating ferroptosis signaling pathway. Biomed Pharmacother 2019; 109: 2043-2053.